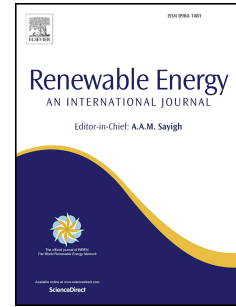


Journal Pre-proof

A modelling evaluation of electromagnetic fields emitted by buried subsea power cables and encountered by marine animals: considerations for marine renewable energy development

Zoë L. Hutchison, Andrew B. Gill, Peter Sigray, Haibo He, John W. King



PII: S0960-1481(21)00717-5

DOI: <https://doi.org/10.1016/j.renene.2021.05.041>

Reference: RENE 15398

To appear in: *Renewable Energy*

Received Date: 21 December 2020

Revised Date: 4 May 2021

Accepted Date: 6 May 2021

Please cite this article as: Hutchison ZL, Gill AB, Sigray P, He H, King JW, A modelling evaluation of electromagnetic fields emitted by buried subsea power cables and encountered by marine animals: considerations for marine renewable energy development, *Renewable Energy*, <https://doi.org/10.1016/j.renene.2021.05.041>.

This is a PDF file of an article that has undergone enhancements after acceptance, such as the addition of a cover page and metadata, and formatting for readability, but it is not yet the definitive version of record. This version will undergo additional copyediting, typesetting and review before it is published in its final form, but we are providing this version to give early visibility of the article. Please note that, during the production process, errors may be discovered which could affect the content, and all legal disclaimers that apply to the journal pertain.

© 2021 Published by Elsevier Ltd.

1 **A modelling evaluation of electromagnetic fields emitted by buried subsea power cables and**
2 **encountered by marine animals: considerations for marine renewable energy development**

3

4 Zoë L. Hutchison^{1,2,3*}, Andrew B. Gill^{4,5}, Peter Sigra⁶, Haibo He⁷, John W. King¹

5

6 ¹School of Biology, University of St Andrews, Fife, Scotland

7 ²Graduate School of Oceanography, University of Rhode Island, USA

8 ³Scottish Association for Marine Science, Scottish Marine Institute, Oban, Scotland

9 ⁴PANGALIA Environmental, Bedfordshire, England, UK

10 ⁵Cefas, Centre for Environment, Fisheries and Aquaculture Science, Suffolk, England, UK

11 ⁶KTH, Royal Institute of Technology, Department of Engineering Mechanics/Marine Engineering,
12 Sweden

13 ⁷Department of Electrical, Computer and Biomedical Engineering, University of Rhode Island, USA

14

15 *Corresponding author:

16 Zoë L. Hutchison, zlh1@st-andrews.ac.uk

1 **A modelling evaluation of electromagnetic fields emitted by buried subsea power cables and**
2 **encountered by marine animals: considerations for marine renewable energy development**

3

4 **Abstract**

5 The expanding marine renewable energy industry will increase the prevalence of electromagnetic
6 fields (EMFs) from power cables in coastal waters. Assessments of environmental impacts are
7 required within licensing/permitting processes and increased prevalence of cables will increase
8 questions concerning EMF emissions and potential cumulative impacts. It is presumed that
9 protecting a cable by burial, may also mitigate EMF emissions and potential impacts on species.
10 Focussing on a bundled high voltage direct current (HVDC) transmission cable, we use computational
11 and interpretive models to explore the influence of cable properties and burial depth on the DC
12 magnetic field (DC-MF) potentially encountered by receptive species. Greater cable pair separation
13 increased the deviations from the geomagnetic field and while deeper burial reduced the deviations,
14 the DC-MF was present at intensities perceivable by receptive species. An animal moving along a
15 cable route may be exposed to variable EMFs due to varied burial depth and that combined with an
16 animal's position in the water column determines the distance from source and EMF exposure.
17 Modelling contextually realistic scenarios would improve assessments of potential effects. We
18 suggest developers and cable industries make cable properties and energy transmission data
19 available, enabling realistic modelling and environmental assessment supporting future
20 developments.

21 **Keywords (6 max):** Cumulative impacts, mitigation, buried cable, EMF propagation, receptor species,
22 species perception

23

24

25 **1. Introduction**

26 The Earth's electromagnetic field (EMF) environment consists of both natural and anthropogenic
27 sources. These EMFs may constitute environmental cues that many organisms detect and respond
28 to throughout their lives [1]. Anthropogenic changes or additions to the EMF environment could
29 alter cues with consequences for receptive animals; changes which will need to be considered by
30 marine management groups and may require mitigation to reduce potential negative effects.

31 A major source of EMFs are subsea power cables (hereafter 'cables'). With the planned expansion in
32 marine renewable energy (MRE; wind, wave, tidal stream) across the world as well as regional,
33 national and international energy transfer, the prevalence of cables in coastal and offshore waters
34 will increase greatly, resulting in EMF emissions becoming more frequent and therefore cumulatively
35 more likely to be encountered by receptive animals. For example, there was 13% growth in ocean
36 energy in 2019, with ambitious targets of 23% annual growth until 2030 [2], while offshore wind
37 energy is expected to quadruple by 2030 [3]. Of particular relevance to the expanding MRE
38 industries, is the permitting and consenting process which has a specific requirement for considering
39 the potential impacts of EMFs on receptive species. Additionally, the formal process requires public
40 and stakeholder consultation often raising concerns regarding EMF effects. The present lack of
41 evidence and poor understanding of the effects, can cause delays as the concerns need to be
42 addressed by reviewing literature, modelling and possibly collecting data. These processes are time
43 consuming and mitigation measures to overcome perceived impacts may be costly. Despite this,
44 EMF emissions from cables within the range of detection of receptive animals remains an
45 understudied topic with regard to the environmental effects of energy transmission [4,5]. A more
46 robust evidence base regarding EMFs and their effects on species is required to better inform the
47 permitting and consenting process and remove barriers to present and future large-scale
48 developments.

49 MRE industries use either alternating current (AC), or direct current (DC) cables, or a combination
50 with transformer stations. The cables are either lower capacity inter-array, or higher capacity export
51 cables. For exports, medium voltage AC cables are only used in small capacity developments close to
52 shore (e.g. <20 km), whereas high voltage AC (HVAC) cables are commonly used for distances 15-50
53 km from shore, and high voltage DC cables (HVDC) are preferable for longer distances [6].
54 Presently, HVAC cables are most common in offshore wind farms (OWFs) however HVDC cable have

55 been used more in the past decade, due to better electrical performance over longer distances [6,7].
56 It is projected that HVDC will become more common as the MRE sector progresses [6]. An
57 assessment of 57 European OWFs (>150 MW) demonstrated that between 2008 and 2019, the
58 turbine power and installation depth as well as the OWF power and distance from shore had
59 increased [6]. Preliminary designs of 20 MW wind turbine generators [8], further suggest increasing
60 demands for higher capacity cables. Together with the increased number of MRE devices it is
61 expected there will be higher intensity cable EMFs over wider spatial scales added to the existing
62 EMF environment. As a result, questions have arisen concerning the spatial extent and intensity of
63 cable EMFs encountered by receptive species and the potential consequences regarding natural EMF
64 cues.

65 Natural EMFs provide ecologically important cues to marine species. The dominant source of natural
66 EMF in the sea is the Earth's geomagnetic field which varies between 25 and 65 μTesla^1 from the
67 equator to the poles [1]. In conductive water bodies, the combination of motion and the
68 geomagnetic field creates motionally induced electric fields, arising from the movement of water
69 bodies or animals through the geomagnetic field. Further biological sources are the bioelectric fields
70 produced by organisms themselves [9]. Receptive species may be either electro-receptive,
71 magneto-receptive, or both. Magneto-sensitive animals are able to detect and respond to very small
72 changes in the intensity (i.e. nT- μT), the angle of inclination, direction of a magnetic field (polarity)
73 and use these geomagnetic cues to aid navigation, using a 'magnetic compass' and/or 'magnetic
74 map' sense [10–13]. These senses may facilitate homing, and short/long-distance migrations, to find
75 ecologically important resources such as shelter, and feeding or reproductive grounds [10,14].
76 Electro-receptive species may be indirectly responsive to geomagnetic cues for the same ecological
77 reasons however they may also be responsive to bioelectric cues important in predator-prey
78 relationships, communication and in finding mates [15]. Such bioelectric fields may be AC or DC,
79 typically low frequency (<1-20 Hz, up to 500Hz), and low intensity fields (nV/cm – $\mu\text{V/cm}$) [9,15].
80 Overall, natural electromagnetic cues are ecologically important to receptive animals throughout
81 their life-cycle, contributing to the successful acquisition of food, survival and reproduction [12,15].
82 For this reason, it is important to understand both the anthropogenic changes to the EMF
83 environment and the perception of EMFs from the vantage point of the receptive species (*sensu* [5]).
84 Understanding EMFs encountered by receptive species, requires knowledge of cable characteristics
85 and their influence on EMF emissions.

¹ 1T is equal to $1\text{kg}\cdot\text{s}^{-2}\cdot\text{A}^{-1}$ (SI Base unit) or 1×10^4 G (Gaussian units)

86 Subsea cables are comprised of layers of materials around a conductive copper or aluminium core.
 87 Cables may occur in different arrangements, with varied layers of insulation depending on the type
 88 and manufacturer (Table 1) [16,17]. The cable shielding with mechanical resistance is typically
 89 comprised of lead and steel [16]. Depending on the cable type and properties, cables can weigh 30-
 90 80 kg/m, with conductor cross-sections from 300 up to 3000 mm², and external diameters of 70-
 91 210 mm [16,18]. Modern applications of subsea cables for floating renewable energy devices have
 92 further dynamic design considerations regarding mechanical loading and the hydrodynamic
 93 environment, particularly with upscaling to HV cables [17,19,20].

94 **Table 1.** Overview of the different types of cables and properties deployed in the marine
 95 environment [16,21]. Modern subsea HVDC cables are typically bipolar, paper insulated or extruded
 96 cables. Note that HVAC cables often use three conductors and that power cables may incorporate
 97 fibre optic cables in the bundle.

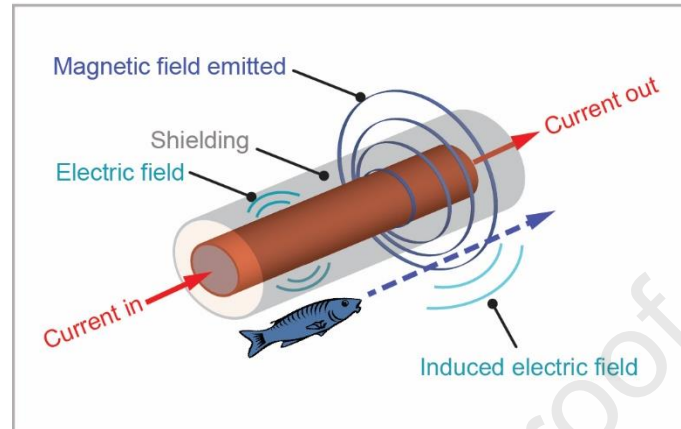
Cable arrangements:	
DC Monopolar	Single-core cable with metallic or sea return Two single core cable with metallic or sea return Concentric cable
DC Bipolar	Two separate single core cables Two single-core cables bundled
AC separate cables	Three single core cables
AC single cables	Three conductors embedded in one cable
Cable types:	Insulation options:
Self-contained fluid filled cables	Self-contained fluid/oil filled (SCFF/SCOF) High pressure fluid/oil filled (HPFF/HPOF) High-pressure gas filled (HFGF)/Gas compression (GC)
Paper insulated (lapped)	Mass impregnated (MI)/Paper insulated lead covered (PILC) Paper polypropylene laminate (PPL)
Extruded cables	Ethylene propylene rubber (EPR) Polyethylene (PE) Cross-linked Polyethylene (XPLE)

98

99 Generally, in a perfectly grounded cable the shielding contains the emitted electric field component
 100 of the EMF, however the magnetic field is emitted into the environment [22]. HVDC cables emit a
 101 static magnetic field (Figure 1), whereas HVAC cables emit a time varying magnetic field, from which
 102 an induced electric field is generated [1]. For both AC and DC cables, an animal or water body
 103 passing through the emitted magnetic field (regardless of AC or DC), creates a motionally induced
 104 electric field (shown for a DC cable in Figure 1) [1]. The intensity of EMF from a cable (DC bipolar,
 105 bundled and AC single cable) decreases approximately as an inverse square of the distance from
 106 source; this attenuation is the same for a cable buried in the seabed, lying uncovered on the seabed
 107 or suspended in the water column (dynamic cables). Furthermore, the properties of the cable

108 shielding, the internal cable arrangement and the power transmitted (voltage applied) all influence
 109 the EMF emitted into the surrounding environment [23,24].

110



111

112 **Figure 1.** A simple representation of a subsea HVDC cable and emitted EMF. The electrical current
 113 passes through the cable conductor. The electric field is contained within the cable shielding, but
 114 the magnetic field is emitted into the surrounding environment. The motionally induced electric
 115 field arising from a fish passing through the emitted magnetic field is also shown. Single-core DC
 116 cables can be paired or bundled with another cable. Note that if the cable were HVAC, an induced
 117 electric field would also be emitted by the transmission of the electrical current. Adapted from [22].

118

119 The majority of subsea cables are bottom mounted. They may be laid on the seabed with hard
 120 protection (rock placement, concrete mattresses, tubular protections) or buried in the seabed, as a
 121 protective measure (e.g. from abrasion or third party damage) [25–27]. Regardless of the external
 122 cable protection, the cable will emit EMFs into the adjacent environment (Figure 1), within
 123 sensitivity ranges known to be perceptible by some animals [12,15]. While the primary function of
 124 burying a cable is to physically protect it [1], there are suggestions of added benefits as a mitigation
 125 measure for potential impacts on animals encountering the cable EMF. This may be stated within
 126 the documentation for environmental impact assessments. However, to be considered in the
 127 context of a potential environmental impact it is necessary to determine how the EMF emitted is
 128 influenced by the cable properties, the burial depth, and the distance of the receptive animal from
 129 the source.

130

131

132 Using previously defined and verified EMF models [28], we modelled the emissions from a HVDC
133 transmission cable under different scenarios to explore the EMF environment likely to be
134 encountered by receptive species. The HVDC cable studied offers (i) a real-world scenario for energy
135 transmission between regions, (ii) a surrogate for high-capacity cables presently used to export
136 energy from OWFs, and (iii) a future outlook for emerging MRE industries. To consider the influence
137 of the cable arrangement, we assessed the degree of cable core separation within a bundled cable,
138 on the level of EMF emitted. Then, with a constant cable separation, we modelled the influence of
139 varying the burial depth on the EMF intensity emitted at the level of the seabed. Building contextual
140 relevance applicable to environmental assessment of EMF effects and the management of MRE and
141 power transmission industries, we provide conceptual interpretations of how EMF emissions may
142 vary for the receptive species with regard to their distance from the cable and the variation in EMF
143 along a cable route.

144

145 **2. Methods**

146 A model previously developed and verified was employed here using the commercially available
147 COMSOL Multiphysics® software (hereafter, 'COMSOL model') [28]. The model and parameters used
148 are described in brief, and readers are referred to Hutchison et al., (2020) for full details of the
149 model and its empirical verification. Hereafter, we refer to the modelled DC magnetic field emitted
150 from the HVDC cable as the 'DC-MF', deliberately differentiating from the EMF which is a broader
151 reflection of electromagnetic field components in both the anthropogenic and natural context.

152 The model was built based on the properties of the subsea Cross Sound Cable (CSC) which is a 40 km
153 HVDC domestic supply cable buried in Long Island Sound, USA (41.223563, -72.900229). The CSC is a
154 bipolar cable which has two single-core cables bundled together. The highest nominal current was
155 1175 A (330 MW, 300 kV). This is comparable to the power transmission characteristics of a HVDC
156 OWF export cable. The model was previously verified using *in situ* measurements of the EMF
157 emitted from the CSC and the application of the model to a higher capacity cable was also verified
158 (1320 A, 600 MW, 500 kV, Neptune Cable, New Jersey, USA). The COMSOL software modelled the
159 DC-MF emitted from the CSC based on the physical details of the real-world environment, including
160 the structural, morphological components, and material properties of the cable and the local
161 geomagnetic field specific to the CSCs location (Table 2). This model was used to provide a detailed

162 and accurate prediction of the DC-MF at the level of the seabed and in the water column above the
163 cable.

164 Within COMSOL, a Free Tetrahedral mesh was applied to the whole domain. The quadrilateral mesh
165 consisted of 17952 domain elements and 1499 boundary elements with increased density close to
166 the cables to accommodate the close-range variation in intensity. The permittivity ϵ (F/m) and
167 permeability μ (H/m) for each of the cable materials were derived by $\epsilon = \epsilon_r \cdot \epsilon_0$ and $\mu = \mu_r \cdot \mu_0$ where ϵ_0
168 and μ_0 are the permittivity (8.8542×10^{-7} F/m) and the permeability ($4\pi \times 10^{-7}$ H/m) of vacuum. For
169 each cable material the relatively permittivity (ϵ_r) and relative permeability (μ_r) are reported in Table
170 2. Using the Cartesian coordinate system, the model was built where the x-axis orients to the
171 northeast, the y-axis to the vertical direction of the earth and the cable lay on the z-axis. Within this
172 local coordinate system, the geomagnetic field components, y corresponds to $-47\mu\text{T}$, and as
173 calculated from vector decomposition, x corresponds to $10.6\mu\text{T}$ and z to $-17.7\mu\text{T}$. Therefore, the
174 corresponding local geomagnetic flux density is $(B_x^b, B_y^b, B_z^b) = (10.6, -47, -17.7)\mu\text{T}$, and the background
175 magnetic field is approximately $51.3\mu\text{T}$. The magnitude of the total magnetic field was calculated by;
176 $\|B_{\text{tot}}\| = \sqrt{(B_x^b + B_x)^2 + (B_y^b + B_y)^2 + (B_z^b)^2}$.

177 Using the 2D AC/DC module, the cable EMF was simulated using three equations. The magnetic field
178 intensity (H) was used to derive the current density (J); $\nabla \times H = J$. The magnetic flux density (B) was
179 derived from the magnetic vector potential (A); $B = \nabla \times A$. The current density (J) and magnetic flux
180 density (B) could then be used to solve; $J = \sigma E + \sigma v \times B + J_e$, where σ is the electrical conductivity
181 (Table 2), E is the electric field intensity, v is the velocity of the conductor and J_e is the externally
182 generated current density. The equations were solved with a numerical iteration algorithm using a
183 flexible generalised minimal residual method with a relative error tolerance of 0.001 and initial value
184 of $A = 0$. The model converged and was used to produce baseline models of the EMF emitted from
185 the CSC (Supplementary Figures 1 and 2).

186

187 **Table 2.** An overview of the layers of information incorporated in the COMSOL model. This includes
188 the CSC properties and environmental characteristics for the base model as well as the electrical
189 conductivity, relative permittivity, and relative permeability for each material. *Note that the
190 standard distance between the bundled cables and the burial depth are provided as initially
191 developed but were varied for the application in this paper.

Layers	Details	Electrical conductivity σ (s/m)	Relative permittivity ϵ_r	Relative permeability ϵ_0
HVDC cable*	Bipolar (bundled cable pair, separation distance 0.106 m)	-	-	-

Conductor	Copper, radius 0.053 m	5.8e7	1.0	1.0
Sheath	Lead, radius 0.041 m	1e6	1.0	1.0
Insulator	XLPE	0	2.3	1.0
Armour	Steel wire, thickness 0.01 m	1.1e6	1.0	1000
Water	Ocean, 35 ppt	1.0	81.0	1.0
Seabed*	Sediment, 1.5 m burial depth	0.24	25.0	1.0
Geomagnetic field	Vertical (47 μ T), North (20 μ T), East (-5 μ T)	-	-	-

192

193 The COMSOL model was used to predict the DC-MF emitted, and how it varies due to (i) the
 194 separation distance between the two bundled cables and (ii) variable burial depth. Firstly, with a
 195 constant burial depth of 1.5 m, the DC-MF emitted at the level of the seabed-water interface was
 196 modelled with a cable separation distance varying between 0.106 and 0.689 m (centre to centre).
 197 Secondly, with a constant cable separation of 0.106 m, the DC-MF emitted at the level of the
 198 seabed-water interface was modelled for the CSC buried at depths varying from 0.6 to 1.8 m, in
 199 0.2 m increments. In both cases, the DC-MF emitted at the level of the seabed-water interface is
 200 reported in terms of the corresponding maximal positive and maximal negative deviation from the
 201 local geomagnetic field of 51.3 μ T (Supplementary Figure 1).

202 Lastly, to demonstrate the cable DC-MF emissions as they would be presented to a receptive species
 203 in the marine environment, two conceptual models were built. The first, demonstrates the
 204 fluctuation in the cable DC-MF intensity that an animal may experience moving along a cable route,
 205 at the level of the seabed-water interface. The second demonstrates the change in DC-MF exposure
 206 that a receptive animal would experience with increasing distance from the seabed using the
 207 computed model (Supplementary Figure 1 and 2).

208 3. Results

209 An asymmetry in the DC-MF on either side of the cable occurred (Supplementary Figure 1) due to
 210 the asymmetrical convolution with Earth's magnetic field, and for this reason, the maximal positive
 211 and negative deviations from the local geomagnetic field for each scenario are reported as the
 212 magnetic flux density.

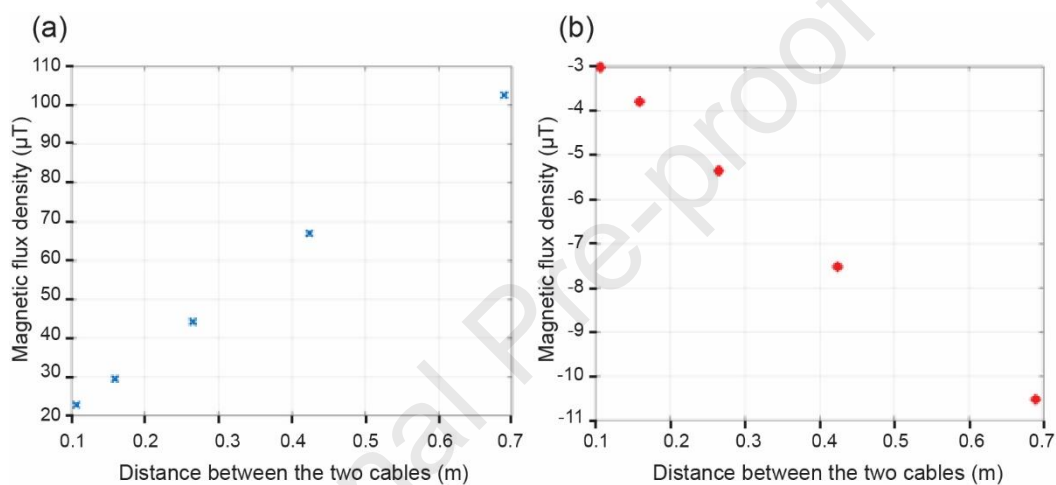
213

214 3.1. Cable Separation Distance

215 In the baseline model the two bundled cables were placed in the horizontal plane and as a result the
 216 positive deviation in the DC-MF on one side of the cable was larger than the negative deviation on

217 the other side of the cable (i.e. asymmetrical, see Supplementary Figure 1). In subsequent models
 218 under the different scenarios, this relationship is maintained. The positive and negative deviations
 219 in the DC-MF are proportional to the separation distance between the two bundled cables (Figure 2a
 220 & b). The magnitude of the DC-MF increased for both the positive and negative deviation, as the
 221 distance between the bundled cables increased. However, the magnitude of change is different. For
 222 example, comparing a cable separation of 0.106 and 0.160 m, the positive deviation (Figure 2a)
 223 changes from 22.7 to 29.5 μT which is a 6.8 μT difference, whereas the negative deviation (Figure
 224 2b) changes from -3.0 to -3.8 μT which is a 0.8 μT difference.

225



226

227 **Figure 2. Influence of the separation distance between bundled cables on the DC magnetic field.**

228 The positive (a) and negative (b) deviation from the local geomagnetic field, as influenced by the
 229 degree of separation between bundled cables (centre to centre). The emitted DC-MF is reported as
 230 the magnetic flux density.

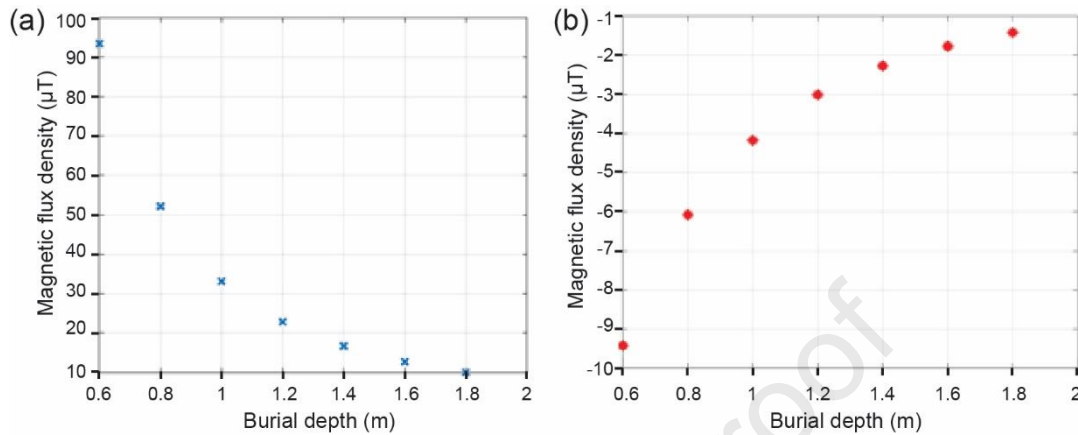
231

232 3.2. Variation in Burial Depth

233 The model of the DC-MF at the level of the seabed-water interface, with constant cable parameters
 234 but variable burial depth, demonstrates a decreasing magnitude of DC-MF emission as the burial
 235 depth increases (Figure 3a & b). The relationship is similar for both the positive and negative
 236 deviation from the geomagnetic field; an increase in burial depth reduces the maximum intensity of
 237 the distortion but again, the magnitude of change is different. For example, comparing a burial
 238 depth of 0.6 and 0.8 m, the positive deviation (Figure 3a) changes from 93.2 to 52.0 μT which is a
 239 41.2 μT difference, whereas the negative deviation (Figure 3b) changes from -9.4 to -6.1 μT which is

240 a 3.3 μT difference. The DC-MF is undisturbed by the sediment properties, in both the water column
 241 and in the sediments, since the sediment is non-magnetic.

242



243

244 **Figure 3. The influence of burial depth on the DC magnetic field.** The positive (a) and negative (b)
 245 deviation from the geomagnetic field, as influenced by the burial depth of the cable. The emitted
 246 DC-MF is reported as the magnetic flux density.

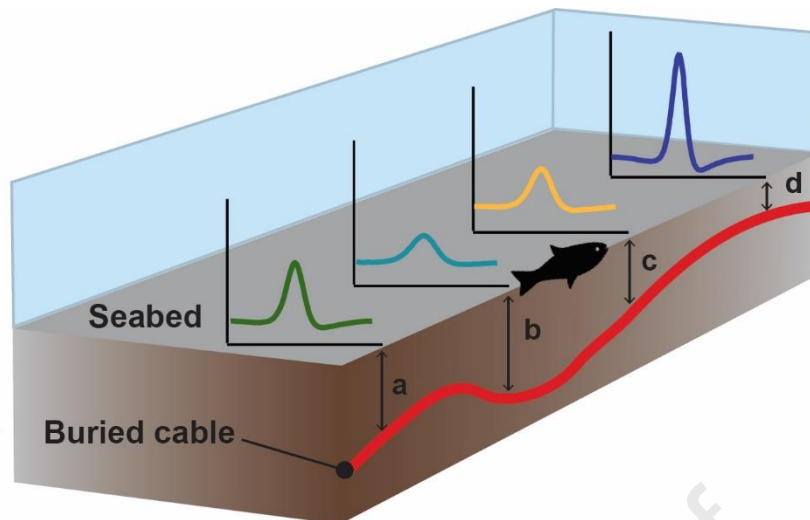
247

248 3.3. Interpretive Models of the DC-MF Presentation to a Receptive Species

249 Many receptive species are mobile entities, and their movement plays a role in the EMF intensity
 250 they will be exposed to. To demonstrate the cable DC-MF emissions as they would be presented to a
 251 receptive species in the marine environment, the baseline models (Supplementary Figure 1 and 2)
 252 with a constant bundled cable separation of 0.106 m and burial depth of 1.5 m, were used to build
 253 interpretive models. These models report the total magnetic field (geomagnetic field plus the
 254 maximal positive distortion).

255 The first scenario incorporates the third dimension and demonstrates the emitted DC-MF intensity
 256 that an animal may experience moving along a cable route. Figure 4 demonstrates the fluctuation in
 257 the emitted DC-MF intensity at the level of the seabed-water interface. The emitted DC-MF is
 258 depicted as the total magnetic field with the assumption of a stable geomagnetic field (51.3 μT).

259

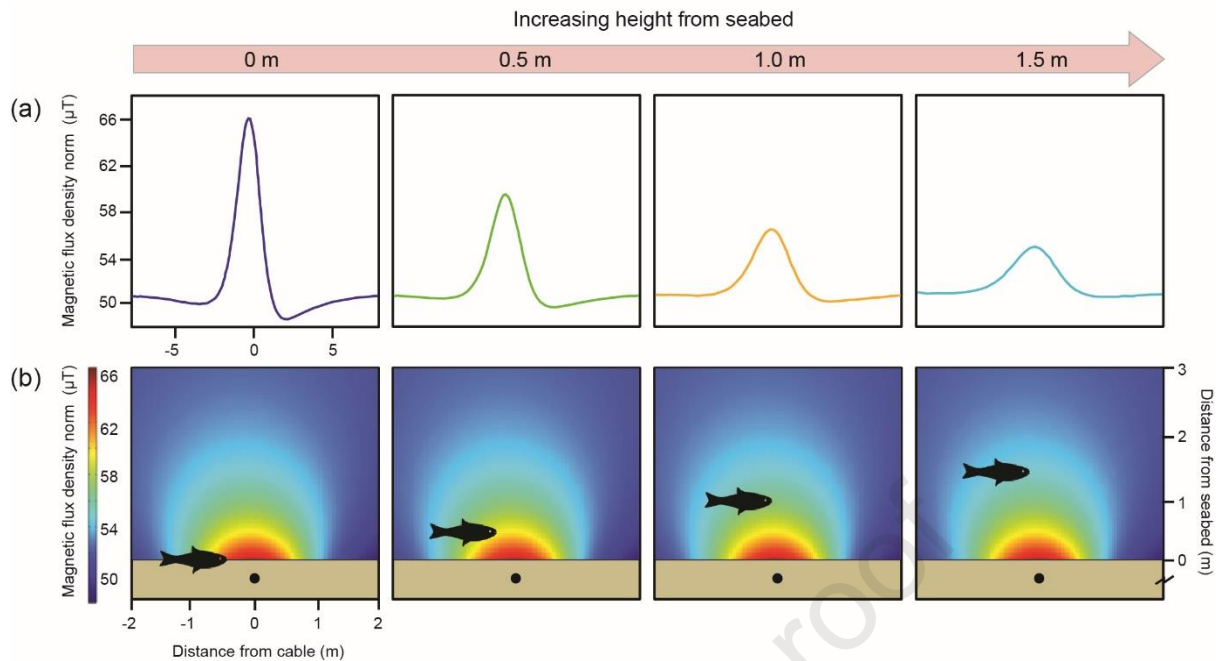


260

261 **Figure 4. Exposure of a receptive species to the emitted DC magnetic field, relative to the animal's**
 262 **movement along a cable route.** The cable burial depth may vary along a cable route due to
 263 different burial depths. For a species moving along the seabed, the variable burial depth of the
 264 cable, changes the distance from source and exposes the animal to variable DC-MF intensities.
 265 Burial depths depicted are approximations and not to scale; (a) 2.0 m, (b) 3.0 m, (c) 2.5 m, (d) 1.5 m.

266

267 The second interpretative model considers the vertical movement of the receptive species in the
 268 water column directly above the buried cable. Figure 5 demonstrates an animal positioned at the
 269 seabed-water interface and then at increasing distances above the seabed, in 0.5 m steps. Where
 270 the animal is positioned at the seabed-water interface, the animal would experience the maximum
 271 emitted DC-MF intensity possible in this scenario, which is $14.7 \mu\text{T}$, a total field of $66 \mu\text{T}$ (Figure 5,
 272 first panel). The animal cannot get closer to the cable due to the physical barrier provided by the
 273 seafloor and is a total of 1.5 m from the cable. As the animals moves further into the water column,
 274 the animal is still exposed to the DC-MF. Even at 1.5 m above the seabed, which is a total of 3 m
 275 from the cable, the animal is exposed to a DC-MF within the sensitivity range known to be
 276 perceptible by some animals. The change in the horizontal spatial extent of the emitted DC-magnetic
 277 field can also be observed in Figure 5.



278

279 **Figure 5. Exposure of a receptive species to the emitted DC magnetic field, relative to the animal's**
 280 **position in the water column.** The total magnetic flux density norm (cable DC-MF plus geomagnetic
 281 field) is shown as a line graph (a) and as a density distribution (b), with increasing distance from the
 282 seabed moving from left to right. The cable was buried at 1.5 m in the seabed and the local
 283 geomagnetic field was 51.3 μT . The fish is representative of any receptive species and is not to scale.

284

285 4. Discussion

286 The planned expansion of the marine renewable energy (MRE) industries and the need for energy
 287 transfer between regions will increase the prevalence of electromagnetic fields (EMFs) emitted by
 288 subsea cabling in coastal and offshore waters [2,3,6]. Presently, high voltage alternating current
 289 (HVAC) cables are the most prevalent MRE cable type, with fewer high voltage direct current (HVDC)
 290 cables in use for OWF energy exports [6]. With technological advancements, greater power
 291 production and increasing distances from shore, a move towards the increased use of HVDC is
 292 expected [6,29]. While this is a present scenario for OWFs, it is a future outlook for emerging
 293 industries such as wave and tidal stream energy conversion. With greater cable deployment the
 294 potential for marine species to encounter cable emitted EMFs rises. Although the potential
 295 consequences of EMF encounters remain poorly understood for the subsea cables [4,5], there is
 296 growing evidence that marine species can respond to cable EMFs [28,30,31]. There have been
 297 suggestions that burying a cable will negate potential effects in animals encountering cable EMFs. In
 298 response to this knowledge gap we modelled the EMF using data from an existing bundled HVDC

299 transmission cable (the Cross Sound Cable, CSC, Long Island Sound, USA) to investigate the influence
300 of cable separation distances and the relationship between cable burial and a receptive species.

301 An asymmetrical total field resulted from the superimposition of the three-dimensional cable
302 emitted DC-MF field on the three-dimensional geomagnetic field [28]. The modelling demonstrated
303 that the change in magnitude of the asymmetrical DC magnetic field (DC-MF) was proportional to
304 the separation distance between the bundled cables. At the maximum burial depth modelled (1.8
305 m), the DC-MF remained present at the level of the seabed. With increasing burial depth, the
306 magnitude of the DC-MF was shown to decrease, with both positive and negative deviations from
307 the local geomagnetic field. To contextualise the modelling regarding a receptive species encounter
308 with cable EMFs, we demonstrated the change in EMF intensity that an animal on the seabed may
309 experience when moving along a cable route with varying cable burial depths. We further
310 demonstrated that the EMF encountered by a receptive species, varies with the animal's proximity
311 to the cable, which is determined by both an animal's position in the water column and the cable
312 burial depth. Our results highlight the importance of understanding how the cable characteristics
313 influence the EMF emitted as well as the context of how an animal may encounter a cable EMF.

314 **4.1. Cable Properties Influence the Emitted EMF**

315 The separation distance between cables bundled together is one example of how cable properties
316 will influence the emitted EMF. Each cable current generates a stationary magnetic field and if
317 perfectly overlapped, the magnetic fields will cancel each other. For the CSC, bundling the cables did
318 not result in DC-MF cancellation. However, cables bundled closer to each other reduced the
319 magnitude of the DC-MF for both the positive and negative deviation from the geomagnetic field
320 indicating a degree of cancellation (Figure 2). For bipolar cables in general, spatial arrangements of
321 cables may vary due to the way that cables are bundled together, or due to different cable external
322 diameters [16]. Closer spatial arrangements may reduce the deviation from the geomagnetic field,
323 but the variable shielding would need to be considered in models of other cables (Table 1). The
324 properties of shielding used in a cable may further influence the emitted DC-MF (permittivity,
325 conductivity and permeability [23,24]) or additional armour where the cable is required to withstand
326 mechanical stress [27]. The extent of cable separation modelled in this paper (0.689 m maximum,
327 Figure 2) exceeds what is likely for bundled cables. In scenarios where bipolar cables are deployed
328 as two individual cables, the degree of separation is broader owing to water depth and allowing
329 cables to be safely accessed in the event of cable fault or maintenance [26,32]. Other cable
330 properties which influence the EMF emitted from a bundled cable is the rotation of the cable pair as
331 they are deployed into or onto the seabed and the orientation of the emitted EMF to the

332 geomagnetic field [28]. Additionally, three-core AC cables have magnetic fields that are 120° out of
333 phase and emit a rotating induced electric field into the environment [24]. Furthermore, helically
334 twisted AC cables, reduces the magnetic field generated and therefore the induced electric field,
335 compared to three straight concentric conductors [33].

336 **4.2. Cable Burial Does Not Eliminate the Emitted EMF**

337 The model of the CSC showed an increasing intensity of DC-MF at the seabed surface with shallower
338 burial depth (i.e. closer proximity to the source) (Figure 3). Bottom fixed cables are buried for their
339 protection from abrasion, fishing activities and other maritime use of the area [27]. The techniques
340 used for burial (e.g. jetting, ploughing, cutting) and depths of burial obtained are dependent on the
341 seabed type and the type of fishing activity in the area [34]. A Burial Protection Index takes account
342 of these factors and guides the most suitable burial depth [27,34,35]. However, a balance of
343 mitigating risk to the cable and achieving economical burial may result in variable target burial
344 depths [27](e.g. deeper burial in a shipping lane). The realised burial depths may also vary owing to
345 the seabed properties (e.g. geological deposits unknown at the planning stage) in which case the
346 installation process adopts the principles of reasonable endeavour, distinguishing between minimum
347 and target burial depths [27]. Once buried, natural erosion may reduce the burial depth or may
348 expose portions of the cable [35], leading to further variation in burial depths along a cable route.

349 Variable burial depth along a cable route results in a changing intensity of EMF experienced by a
350 receptive animal on the seabed (Figure 4). Species may encounter cable EMFs each time they cross
351 over the cable route or they may follow the cable route. The change in EMF intensity is a function
352 of distance from source. Therefore, while we explain the EMF variation due to different burial
353 depths, a change in proximity to the cable may also result from other cable protections used, even
354 along the same cable [5,27]. For example, the Wave Hub (UK) 25 km export cable is buried in soft
355 sediment within 7 km of shore, and beyond that has rock armouring (0.3 m deep) with concrete
356 mattresses at 120 m intervals [36]. The Paimpol-Brehat tidal test site (France) similarly has 4 km of
357 buried cable close to shore and 11 km of unburied cable protected with concrete mattresses (0.3 m
358 deep blocks) at approximately 50 m intervals [37]. In both cases, the maximum increase in distance
359 from the EMF source due to the unburied cable protection is 0.3 m. Furthermore, the protection
360 provides hard substrate to be colonised by species and structural heterogeneity offering crevices for
361 animals to live in [36,37], which may increase the likely encounter of EMF and allow animals to get
362 closer than 0.3 m from the cable. This highlights that the animal's proximity to the cable, regardless
363 of protection is a key factor in their exposure to EMFs (Figure 5). The frequency of an encounter, i.e.
364 the encounter rate, is also important in the context of cumulative effects. Laboratory studies of

365 exposure to electric fields have shown the capacity of a receptive species to learn, habituate and
366 retain only short-term memory of experiences [38]. This observation implies that reinforcement is
367 required for an experience to be memorised for a longer period and if MFs are variable due to
368 variable protection and an animal's proximity to the cable, longer term memory of an encounter
369 may not be supported.

370 Spatial configurations of cables are also important in the context of an animal's encounter. The
371 movement of animals within an array of MRE devices may provide further variation in the
372 encountered EMF due to varied cable size and increasing power generation between interconnected
373 devices [39]. In the case of offshore wind arrays, inter-array cable configurations (topology) may be
374 radial, star or loop designs and future optimization, required due to growing capacity arrays, may
375 consider the topology as well as cable size and number of substations to minimise power losses and
376 installation expenses [40,41]. Furthermore, arrays of floating wind or suspended wave and tidal
377 devices introduce unprotected dynamic cables into the water column [17,19,29], presenting EMFs to
378 pelagic species. Such EMF scenarios experienced by benthic and pelagic species, may become more
379 complex with the advancement of co-location and multi-use platforms [42]. Furthermore, multiple
380 arrays in a region may have export cables which cross paths, share a common cable corridor, or
381 energy collection platforms/systems may be used facilitating connection to the grid through a
382 common higher capacity cable [5].

383 **4.3. Understanding Animal Interactions with EMFs**

384 When considering cable EMFs it is important to take account of movement ecology for both benthic
385 and pelagic species as the likely encounter of a cable EMF may change during the lifecycle of the
386 receptive species [5]. For buried cables, the proximity of an animal to the seabed is a contributing
387 factor to the distance from source and will influence the intensity of EMF the animal is exposed to
388 (Figure 5). For example, demersal species often swim in the water column and pelagic species may
389 come into contact with the EMF owing to their use of seabed habitats [5]. Important use of benthic
390 habitats by pelagic species are exemplified by herring spawning on coastal gravel beds [43] and cod
391 using benthic feeding grounds [44]. The movements between pelagic and benthic zones may change
392 by the hour, day or over the longer term, such as seasonally. Use of benthic habitats varies
393 throughout a species lifecycle as can the perception and/or ecological relevance of natural EMF cues
394 which are in the same range as cable EMFs [12,15]. For example embryonic skates and rays can
395 detect bioelectric cues from predators facilitating survival and later, as mature adults bioelectric
396 cues are used to forage and find mates [45,46]. In the Caribbean spiny lobster (*Panulirus argus*),
397 demonstrated to use the geomagnetic field in homing [14], a similar developmental shift in

398 responses to magnetic fields has been proposed [47]. Salmonids and anguillids also use the
399 geomagnetic field to orientate during early life-history and adult migrations [48–50]. Since species
400 obtain cues from natural EMFs differently at different stages of their life, it is reasonable to expect
401 that their responses to cable EMFs may also differ.

402 Cable EMFs may interact with important natural cues obtained from small-scale changes in the local
403 geomagnetic field. For example, local geomagnetic imprinting has been shown in sockeye salmon
404 (*Oncorhynchus nerka*) and it is proposed that they use the small differences in geomagnetic intensity
405 as an environmental cue during homing to their natal rivers for spawning [50]. Gradual drift of the
406 geomagnetic field with annual differences ranging from 138 to >200 nT influenced the diversion rate
407 of migrating salmon [50]. Similarly small-scale changes in the geomagnetic field intensity (4.9%) and
408 inclination angle (3.0%) have been demonstrated to influence the orientation of juvenile European
409 eels (*Anguilla anguilla*) [51], and elasmobranchs were able to detect and respond to artificial field
410 gradients ranging from 25 to 100 μ T, relative to an ambient field of 36 μ T [52]. These studies
411 highlight that very low intensity changes in the geomagnetic field used by animals, can be both
412 positive and negative. For the CSC modelled here, the EMF was an asymmetrical field with variable
413 positive and negative deviations from the geomagnetic field. The relationships between burial
414 depth and the positive and negative deviation of the DC-MF were not linear and furthermore the
415 total intensities experienced by an animal, differ with their proximity to the cable. Despite a lower
416 intensity EMF at greater distance from the cable, the change from the ambient geomagnetic field,
417 which may be a higher or lower total field, may still present distortions of the local geomagnetic field
418 that species respond to. For example, in Figure 5, at 1.5 m above the seabed (3 m from source) the
419 magnetic field changes by approximately 3 μ T (3000 nT) and is within the expected perceptive range
420 of a receptive species. Aside from the change in EMF intensity, orientation of the cable to the
421 geomagnetic field and potential distortion of the inclination should be a further consideration.
422 There is growing evidence that species may be responsive to the angle of inclination of the
423 geomagnetic field (e.g. turtles [53,54], salmon [50,55], eels [56], elasmobranchs [13]) and feasibly
424 may be responsive to the angle of declination [11]. It is important that we take the vantage point of
425 the receptive species to understand how species perceive the EMF environment and how cable
426 EMFs may change the cues ecologically important in the acquisition of food, survival and
427 reproductive success [5].

428 **4.4. The Need to Consider EMF Cumulative Effects**

429 Energy transmission is a major component of MRE developments [57], applicable to fixed and
430 floating devices and multi-platform or co-location designs (e.g. [42]). Presently, EMF emissions are

431 considered in the planning and licensing/permitting process as a potential operational
432 environmental impact. Cumulative impacts, where combined incremental effects (which may be
433 considered minor alone) pose a greater likelihood of impact on marine life are also considered [58].
434 Concerns regarding cumulative EMF impacts will increase with the growth of MRE industries and a
435 greater prevalence of energy generation and power transmission in the sea. Action now, in the form
436 of data availability, EMF model verification with empirical measurements and targeted research on
437 species effects and impacts, will support the development of these industries at larger scales in
438 future.

439 Concerns regarding EMF impacts are typically scoped out at an early stage, often stating that the
440 cable will be buried (inferred as mitigation), and the emitted EMF is modelled to be below the
441 geomagnetic field (25 to 65 μT) or nearly cancelled due to cable properties. However, the models
442 demonstrate that EMF emissions are not eliminated by cable burial (Section 4.2). Furthermore, our
443 knowledge has advanced to determine that species respond to very low intensity changes (i.e. nT-
444 μT) and inclination of the geomagnetic field (Section 4.3). We now have empirical measurements of
445 EMFs in similar ranges from buried cables [28,59], including those that are considered to have a
446 degree of self-cancellation [60]. Empirical evidence of species responding to cable EMFs also exists
447 [28,30,31]. Based on such modern evidence, it is not appropriate to dismiss the EMF emissions as
448 being below background levels, the interaction of the cable emitted EMF and local geomagnetic field
449 must be considered, together with physical variations along cable routes and temporal variability in
450 energy transmission. The present knowledge base available to determine if there is an impact on
451 species is lacking both in terms of the characterisation of EMFs (physical) and how species respond
452 to them (biological/ecological) [5]. The evidence indicates that EMF should be explored further, and
453 be a cumulative impact consideration for future large-scale developments, particularly where
454 multiple cables occur in a given region [61].

455 Modelling is a standard approach for determining the EMF emissions from AC and DC cables [62].
456 However, models are 2D idealised scenarios which are rarely supported by empirical in situ
457 measurements. The model used in this study is also a 2D scenario of the DC-MF emitted from the
458 CSC and while demonstrated to be representative of the DC-MF, it is known to be an underestimate
459 and oversimplification of the full EMF emissions. Empirical measurements of the CSC revealed
460 different shape signatures of the emitted DC-MF along the cable route due to the interaction with
461 the geomagnetic field, and unexpected AC fields (magnetic and electric) were associated with the DC
462 CSC and other DC cables [28]. Yet, the application of the model in this study was suitable for
463 analysing the emitted DC-MF under the different scenarios selected. While empirical measurements
464 of deployed subsea cables are essential to improve the knowledge base, they would likely be

465 considered an excessive burden on developers [63], particularly where there is no standardised
466 methodology for measuring and reporting EMFs [4,5]. Laboratory measurements may provide
467 verifications for some aspects relating to operational cable properties in the absence of
468 environmental influences. To reduce uncertainty about the environmental impact of EMFs and to
469 validate the knowledge from modelling, a combined approach is needed and is reliant on data
470 availability. Models can be applied to more contextually relevant, realistic scenarios which better
471 inform on the likely EMFs emitted and verified through empirical measurements of EMFs from
472 different cable types, orientations and configurations. Relevant cable property information and
473 temporal energy transfer data being readily available and accessible would facilitate these goals.
474 Subsequently, a fuller understanding of the EMFs presented to species will follow enabling improved
475 assessments of environmental effects and impacts. This approach will either inform us that the risk
476 can be retired (*sensu* [61]) with a degree of confidence for cable scenarios or that appropriate
477 mitigations are necessary, ultimately reducing future barriers to development.

478 **5. Conclusions and Recommendations**

479 This study demonstrates the need to consider cable properties and the position of the cable in the
480 environment (including burial) with respect to how the emitted DC-MF is presented and
481 encountered by receptive species. We focused on a bipolar bundled HVDC cable since they are
482 representative of modern installations and are expected to become more common in future
483 [6,21,29]. However, the model presented only addressed the DC component of the emitted EMF
484 and through empirical measurements of the CSC cable and others, it is known that AC fields may be
485 associated with HVDC cables, extending greater spatial ranges than the DC magnetic field [28]. Going
486 forward, models should be expanded to include all aspects of the EMF (DC and AC, magnetic and
487 electric fields) which would be better informed by empirical characterizations [1]. Greater
488 contextual relevance of the EMF presented to receptive species could also be obtained by
489 incorporating temporal changes in the power transmission [28] and variability of the cables position
490 in the marine environment. This approach is of particular importance as fixed and dynamic cables
491 become more frequent and present EMFs at different orientations within the water column and/or
492 as more advanced configurations in the marine environment [17,40]. Incorporation of these
493 recommendations into future EMF models would improve their contextual relevance, further
494 supporting assessments of the potential effects of receptive species however, this must be coupled
495 with a better understanding of how a receptive species may encounter and respond to cable EMFs
496 [5].

498 **References**

- 499 [1] A.B. Gill, I. Gloyne-Philips, J. Kimber, P. Sigray, Marine renewable energy, electromagnetic
500 (EM) fields and EM-sensitive animals, in: M.A. Shields, A.I.L. Payne (Eds.), *Mar. Renew. Energy*
501 *Technol. Environ. Interact.*, Springer Netherlands, Dordrecht, 2014: pp. 61–79.
502 https://doi.org/10.1007/978-94-017-8002-5_6.
- 503 [2] IEA, *Ocean Power*, Paris; France, 2020. <https://www.iea.org/reports/ocean-power>.
- 504 [3] IEA, *Offshore Wind Outlook 2019*, Paris, France, 2020. [https://www.iea.org/reports/offshore-](https://www.iea.org/reports/offshore-wind-outlook-2019)
505 [wind-outlook-2019](https://www.iea.org/reports/offshore-wind-outlook-2019).
- 506 [4] A.B. Gill, M. Desender, Risk to Animals from Electromagnetic Fields Emitted by Electric Cables
507 and Marine Renewable Energy Devices, in: A.E. Copping, L.G. Hemery (Eds.), *OES-*
508 *Environmental 2020 State Sci. Rep. Environ. Eff. Mar. Renew. Energy Dev. Around World,*
509 *Report for Ocean Energy Systems (OES)*, 2020: pp. 86–103. <https://doi.org/10.2172/1633088>.
- 510 [5] Z.L. Hutchison, D.H. Secor, A.B. Gill, The interaction between resource species and
511 electromagnetic fields associated with electricity production by offshore wind farms,
512 *Oceanography*. 33 (2020) 96–107. <https://doi.org/10.5670/oceanog.2020.409>.
- 513 [6] E.P.P. Soares-Ramos, L. de Oliveira-Assis, R. Sarrias-Mena, L.M. Fernández-Ramírez, Current
514 status and future trends of offshore wind power in Europe, *Energy*. 202 (2020) 117787.
515 <https://doi.org/10.1016/j.energy.2020.117787>.
- 516 [7] A. Kalair, N. Abas, N. Khan, Comparative study of HVAC and HVDC transmission systems,
517 *Renew. Sustain. Energy Rev.* 59 (2016) 1653–1675.
518 <https://doi.org/10.1016/j.rser.2015.12.288>.
- 519 [8] L. Sartori, F. Bellini, A. Croce, C.L. Bottasso, Preliminary design and optimization of a 20MW
520 reference wind turbine, *J. Phys. Conf. Ser.* 1037 (2018) 42003. [https://doi.org/10.1088/1742-](https://doi.org/10.1088/1742-6596/1037/4/042003)
521 [6596/1037/4/042003](https://doi.org/10.1088/1742-6596/1037/4/042003).
- 522 [9] C.N. Bedore, S.M. Kajiura, Bioelectric fields of marine organisms: voltage and frequency
523 contributions to detectability by electroreceptive predators, *Physiol. Biochem. Zool.* 86 (2013)
524 298–311. <https://doi.org/10.1086/669973>.
- 525 [10] K.J. Lohmann, C.M.F. Lohmann, C.S. Endres, The sensory ecology of ocean navigation, *J. Exp.*
526 *Biol.* 211 (2008) 1719–1728. <https://doi.org/10.1242/jeb.015792>.

- 527 [11] G.C. Nordmann, T. Hochstoeger, D.A. Keays, Magnetoreception—a sense without a receptor,
528 PLOS Biol. 15 (2017) e2003234. <https://doi.org/10.1371/journal.pbio.2003234>.
- 529 [12] K. Formicki, A. Korzelecka-Orkisz, A. Tański, Magnetoreception in fish, J. Fish Biol. (2019).
530 <https://doi.org/10.1111/jfb.13998>.
- 531 [13] K.C. Newton, S.M. Kajiura, The yellow stingray (*Urobatis jamaicensis*) can discriminate the
532 geomagnetic cues necessary for a bicoordinate magnetic map, Mar. Biol. 167 (2020) 151.
533 <https://doi.org/10.1007/s00227-020-03763-1>.
- 534 [14] L.C. Boles, K.J. Lohmann, True navigation and magnetic maps in spiny lobsters, Nature. 421
535 (2003) 60–63. <https://doi.org/10.1038/nature01226>.
- 536 [15] K.C. Newton, A.B. Gill, S.M. Kajiura, Electroreception in marine fishes: chondrichthyans, J. Fish
537 Biol. 95 (2019) 135–154. <https://doi.org/10.1111/jfb.14068>.
- 538 [16] M. Ardelean, P. Minnebo, HVDC submarine power cables in the world, European Union, 2015.
539 <https://doi.org/10.2790/95735>.
- 540 [17] K. Grivas, A. Moraiti, G. Georgallis, G. Rinaldi, P.R. Thies, L. Johanning, Dynamic HV cables
541 with AL conductors for floating offshore wind turbines: A cost and behavior comparative
542 study, Dev. Renew. Energies Offshore. (2020) 644–649.
543 <https://doi.org/10.1201/9781003134572-73>.
- 544 [18] European Subsea Cables Association (ESCA), Submarine Power Cables, 2020.
545 <https://www.escae.eu/articles/submarine-power-cables/>.
- 546 [19] P.R. Thies, L. Johanning, C. Dobral, Parametric Sensitivity Study of Submarine Power Cable
547 Design for Marine Renewable Energy Applications, (2017).
548 <https://doi.org/10.1115/OMAE2017-62208>.
- 549 [20] D.K. Spearman, S. Strivens, Phase II Summary Report: Floating Wind Joint Industry Project,
550 London, 2020.
- 551 [21] S.J. Sutton, P.L. Lewin, S.G. Swingler, Review of global HVDC subsea cable projects and the
552 application of sea electrodes, Int. J. Electr. Power Energy Syst. 87 (2017) 121–135.
553 <https://doi.org/10.1016/j.ijepes.2016.11.009>.
- 554 [22] A.B. Gill, M. Bartlett, F. Thomsen, Potential interactions between diadromous fishes of U.K.
555 conservation importance and the electromagnetic fields and subsea noise from marine
556 renewable energy developments, J. Fish Biol. 81 (2012) 664–695.

- 557 <https://doi.org/10.1111/j.1095-8649.2012.03374.x>.
- 558 [23] CMACS, A baseline assessment of electromagnetic field generated by offshore windfarm
559 cables, 2003.
- 560 [24] A.B. Gill, Y. Huang, J. Spencer, I. Gloyne-Philips, Electromagnetic Fields emitted by High
561 Voltage Alternating Current Offshore Wind Power Cables and interactions with marine
562 organisms, Institute of Engineering and Technology, London, 2012.
563 <https://tethys.pnnl.gov/sites/default/files/publications/Gill-2012.pdf>.
- 564 [25] B. Taormina, J. Bald, A. Want, G. Thouzeau, M. Lejart, N. Desroy, A. Carlier, A review of
565 potential impacts of submarine power cables on the marine environment: knowledge gaps,
566 recommendations and future directions, *Renew. Sustain. Energy Rev.* 96 (2018) 380–391.
567 <https://doi.org/https://doi.org/10.1016/j.rser.2018.07.026>.
- 568 [26] F. Dinmohammadi, D. Flynn, C. Bailey, M. Pecht, C. Yin, P. Rajaguru, V. Robu, Predicting
569 Damage and Life Expectancy of Subsea Power Cables in Offshore Renewable Energy
570 Applications, *IEEE Access.* 7 (2019) 54658–54669.
571 <https://doi.org/10.1109/access.2019.2911260>.
- 572 [27] Det Norske Veritas AS, Subsea Power Cables in Shallow Water Renewable Energy
573 Applications; Recommended Practice DNV-RP-J301, 2016. www.dnvgl.com.
- 574 [28] Z.L. Hutchison, A.B. Gill, P. Sigray, H. He, J.W. King, Anthropogenic electromagnetic fields
575 (EMF) influence the behaviour of bottom-dwelling marine species, *Sci. Rep.* 10 (2020) 4219.
576 <https://doi.org/10.1038/s41598-020-60793-x>.
- 577 [29] R. James, W.-Y. Weng, Floating Wind Joint Industry Project; Key Findings from Electrical
578 Systems, Mooring Systems, and Infrastructure & Logistics studies, London, 2018.
- 579 [30] H. Westerberg, I. Lagenfelt, Sub-sea power cables and the migration behaviour of the
580 European eel, *Fish. Manag. Ecol.* 15 (2008) 369–375. [https://doi.org/10.1111/j.1365-
581 2400.2008.00630.x](https://doi.org/10.1111/j.1365-2400.2008.00630.x).
- 582 [31] M.T. Wyman, A. Peter Klimley, R.D. Battleson, T. V Agosta, E.D. Chapman, P.J. Haverkamp,
583 M.D. Pagel, R. Kavet, Behavioral responses by migrating juvenile salmonids to a subsea high-
584 voltage DC power cable, *Mar. Biol.* 165 (2018) 134. [https://doi.org/10.1007/s00227-018-
585 3385-0](https://doi.org/10.1007/s00227-018-3385-0).
- 586 [32] V. Wendt, An Introduction to High Voltage Direct Current (HVDC) Subsea Cable Systems,
587 Brussels, 2012.

- 588 [33] P. Pettersson, N. Schonborg, Reduction of power system magnetic field by configuration
589 twist, *IEEE Trans. Power Deliv.* 12 (1997) 1678–1683. <https://doi.org/10.1109/61.634190>.
- 590 [34] R. Benato, I. Balanuye, F. Köksal, N. Ozan, E. Özdemirci, Installation of XLPE-Insulated 400 kV
591 Submarine AC power cables under the dardanelles strait: A 4 GW Turkish grid reinforcement,
592 *Energies.* 11 (2018) 1–15. <https://doi.org/10.3390/en11010164>.
- 593 [35] Department for Business Enterprise & Regulatory Reform (BERR), Review of Cabling
594 Techniques and Environmental Effects Applicable to the Offshore Wind Farm Industry:
595 Technical Report, 2008.
- 596 [36] E. V Sheehan, A.Y. Cartwright, M.J. Witt, M.J. Attrill, M. Vural, L.A. Holmes, Development of
597 epibenthic assemblages on artificial habitat associated with marine renewable infrastructure,
598 *ICES J. Mar. Sci.* 77 (2020) 1178–1189. <https://doi.org/10.1093/icesjms/fsy151>.
- 599 [37] B. Taormina, M. Laurans, M.P. Marzloff, N. Dufournaud, M. Lejart, N. Desroy, D. Leroy, S.
600 Martin, A. Carrier, Renewable energy homes for marine life: Habitat potential of a tidal
601 energy project for benthic megafauna, *Mar. Environ. Res.* 161 (2020) 105131.
602 <https://doi.org/10.1016/j.marenvres.2020.105131>.
- 603 [38] J.A. Kimber, D.W. Sims, P.H. Bellamy, A.B. Gill, Elasmobranch cognitive ability: using
604 electroreceptive foraging behaviour to demonstrate learning, habituation and memory in a
605 benthic shark, *Anim. Cogn.* 17 (2014) 55–65. <https://doi.org/10.1007/s10071-013-0637-8>.
- 606 [39] M. Fischetti, D. Pisinger, Optimal wind farm cable routing: Modeling branches and offshore
607 transformer modules, *Networks.* 72 (2018) 42–59. <https://doi.org/10.1002/net.21804>.
- 608 [40] M. Sedighi, M. Moradzadeh, O. Kukrer, M. Fahrioglu, Simultaneous optimization of electrical
609 interconnection configuration and cable sizing in offshore wind farms, *J. Mod. Power Syst.*
610 *Clean Energy.* 6 (2018) 749–762. <https://doi.org/10.1007/s40565-017-0366-0>.
- 611 [41] A. Ferguson, P. De Villiers, B. Fitzgerald, J. Matthiesen, Benefits in moving the inter-array
612 voltage from 33 kV to 66 kV AC for large offshore wind farms, in: *Eur. Wind Energy Conf.*
613 *Exhib. 2012, EWEC 2012, 2012:* pp. 902–909.
- 614 [42] K.A. Abhinav, M. Collu, S. Benjamins, H. Cai, A. Hughes, B. Jiang, S. Jude, W. Leithead, C. Lin,
615 H. Liu, L. Recalde-Camacho, N. Serpetti, K. Sun, B. Wilson, H. Yue, B.Z. Zhou, Offshore multi-
616 purpose platforms for a Blue Growth: A technological, environmental and socio-economic
617 review, *Sci. Total Environ.* 734 (2020) 138256.
618 <https://doi.org/10.1016/j.scitotenv.2020.138256>.

- 619 [43] Å.S. Høines, O.A. Bergstad, O.T. Albert, The structure and temporal stability of the fish
620 community on a coastal bank utilized as a spawning ground by herring, *ICES J. Mar. Sci.* 55
621 (1998) 271–288. <https://doi.org/10.1006/jmsc.1997.0268>.
- 622 [44] V.J. Hobson, D. Righton, J.D. Metcalfe, G.C. Hays, Vertical movements of North Sea cod, *Mar.*
623 *Ecol. Prog. Ser.* 347 (2007) 101–110. <https://doi.org/10.3354/meps07047>.
- 624 [45] R.E. Ball, M.K. Oliver, A.B. Gill, Early life sensory ability-ventilatory responses of thornback ray
625 embryos (*Raja clavata*) to predator-type electric fields, *Dev. Neurobiol.* 76 (2016) 721–729.
626 <https://doi.org/10.1002/dneu.22355>.
- 627 [46] J.A. Sisneros, T.C. Tricas, C.A. Luer, Response properties and biological function of the skate
628 electrosensory system during ontogeny, *J. Comp. Physiol. A.* 183 (1998) 87–99.
629 <https://doi.org/10.1007/s003590050237>.
- 630 [47] D.A. Ernst, K.J. Lohmann, Size-dependent avoidance of a strong magnetic anomaly in
631 Caribbean spiny lobsters, *J. Exp. Biol.* 221 (2018) jeb172205.
632 <https://doi.org/10.1242/jeb.172205>.
- 633 [48] F.-W. Tesch, Influence of geomagnetism and salinity on the directional choice of eels,
634 *Helgoländer Wissenschaftliche Meeresuntersuchungen.* 26 (1974) 382–395.
635 <https://doi.org/10.1007/BF01627623>.
- 636 [49] A. Cresci, C.M. Durif, C.B. Paris, S.D. Shema, A.B. Skiftesvik, H.I. Browman, Glass eels (*Anguilla*
637 *anguilla*) imprint the magnetic direction of tidal currents from their juvenile estuaries,
638 *Commun. Biol.* 2 (2019) 1–8. <https://doi.org/10.1038/s42003-019-0619-8>.
- 639 [50] N.F. Putman, K.J. Lohmann, E.M. Putman, T.P. Quinn, A.P. Klimley, D.L.G. Noakes, Evidence
640 for geomagnetic imprinting as a homing mechanism in Pacific salmon, *Curr. Biol.* 23 (2013)
641 312–316. <https://doi.org/10.1016/j.cub.2012.12.041>.
- 642 [51] L.C. Naisbett-Jones, N.F. Putman, J.F. Stephenson, S. Ladak, K.A. Young, A Magnetic Map
643 Leads Juvenile European Eels to the Gulf Stream, *Curr. Biol.* 27 (2017) 1236–1240.
644 <https://doi.org/10.1016/j.cub.2017.03.015>.
- 645 [52] C.G. Meyer, K.N. Holland, Y.P. Papastamatiou, Sharks can detect changes in the geomagnetic
646 field, *J. R. Soc. Interface.* 2 (2005) 129. <https://doi.org/10.1098/rsif.2004.0021>.
- 647 [53] Lohmann, Lohmann, Detection of Magnetic Inclination Angle By Sea Turtles: a Possible
648 Mechanism for Determining Latitude, *J. Exp. Biol.* 194 (1994) 23–32.
649 <http://www.ncbi.nlm.nih.gov/pubmed/9317267>.

- 650 [54] N.F. Putman, C.S. Endres, C.M.F. Lohmann, K.J. Lohmann, Longitude perception and
651 bicoordinate magnetic maps in sea turtles, *Curr. Biol.* 21 (2011) 463–466.
652 <https://doi.org/10.1016/j.cub.2011.01.057>.
- 653 [55] N.F. Putman, M.M. Scanlan, A.M. Pollock, J.P. O’Neil, R.B. Couture, J.S. Stoner, T.P. Quinn, K.J.
654 Lohmann, D.L.G. Noakes, Geomagnetic field influences upward movement of young Chinook
655 salmon emerging from nests, *Biol. Lett.* 14 (2018). <https://doi.org/10.1098/rsbl.2017.0752>.
- 656 [56] L.C. Naisbett-Jones, N.F. Putman, M.M. Scanlan, D.L.G. Noakes, K.J. Lohmann,
657 Magnetoreception in fishes: the effect of magnetic pulses on orientation of juvenile Pacific
658 salmon, *J. Exp. Biol.* (2020) jeb.222091. <https://doi.org/10.1242/jeb.222091>.
- 659 [57] H. Bains, A. Madariaga, M.C.M. Troffaes, B. Kazemtabrizi, An economic model for offshore
660 transmission asset planning under severe uncertainty, *Renew. Energy.* 160 (2020) 1174–1184.
661 <https://doi.org/10.1016/j.renene.2020.05.160>.
- 662 [58] A.D. Judd, T. Backhaus, F. Goodsir, An effective set of principles for practical implementation
663 of marine cumulative effects assessment, *Environ. Sci. Policy.* 54 (2015) 254–262.
664 <https://doi.org/10.1016/j.envsci.2015.07.008>.
- 665 [59] A.P. Klimley, M.T. Wyman, R. Kavet, Chinook salmon and green sturgeon migrate through San
666 Francisco Estuary despite large distortions in the local magnetic field produced by bridges,
667 *PLoS One.* 12 (2017) e0169031. <https://doi.org/10.1371/journal.pone.0169031>.
- 668 [60] Z.L. Hutchison, P. Sigray, H. He, A.B. Gill, J. King, C. Gibson, Electromagnetic Field (EMF)
669 Impacts on Elasmobranch (shark, rays, and skates) and American Lobster Movement and
670 Migration from Direct Current Cables, 2018.
- 671 [61] A.E. Copping, M.C. Freeman, A.M. Gorton, L.G. Hemery, Risk Retirement - Decreasing
672 Uncertainty and Informing Consenting Processes for Marine Renewable Energy Development,
673 *J. Mar. Sci. Eng.* 8 (2020) 172. <https://doi.org/10.3390/jmse8030172>.
- 674 [62] Normandeau Exponent, T. Tricas, A. Gill, E. Normandeau, T. Tricas, A. Gill, Normandeau
675 Exponent, T. Tricas, A. Gill, Effects of EMFs from Undersea Power Cables on Elasmobranchs
676 and Other Marine Species, U.S. Dept. of the Interior, Bureau of Ocean Energy Management,
677 Regulation, and Enforcement, Pacific OCS Region, Camarillo, CA. OCS Study, 2011.
678 [https://www.boem.gov/Environmental-Stewardship/Environmental-Studies/Pacific-](https://www.boem.gov/Environmental-Stewardship/Environmental-Studies/Pacific-Region/Studies/2011-09-EMF-Effects.aspx)
679 [Region/Studies/2011-09-EMF-Effects.aspx](https://www.boem.gov/Environmental-Stewardship/Environmental-Studies/Pacific-Region/Studies/2011-09-EMF-Effects.aspx).
- 680 [63] C.J. Fox, S. Benjamins, E.A. Masden, R. Miller, Challenges and opportunities in monitoring the

681 impacts of tidal-stream energy devices on marine vertebrates, *Renew. Sustain. Energy Rev.*
682 81 (2018) 1926–1938. <https://doi.org/10.1016/j.rser.2017.06.004>.

683

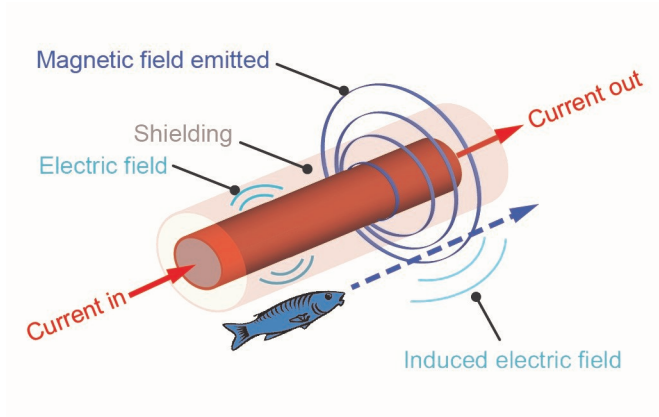
684 **Acknowledgements**

685 Part of this work was supported by the Bureau of Ocean Energy Management (contract number
686 M14PC00009). We thank He Jiang and Yufei Tang (URI) for assistance with modelling and Carol
687 Gibson (URI) for assistance with graphics. We thank the Guest Editors for the invitation to submit an
688 article to this Special Issue.

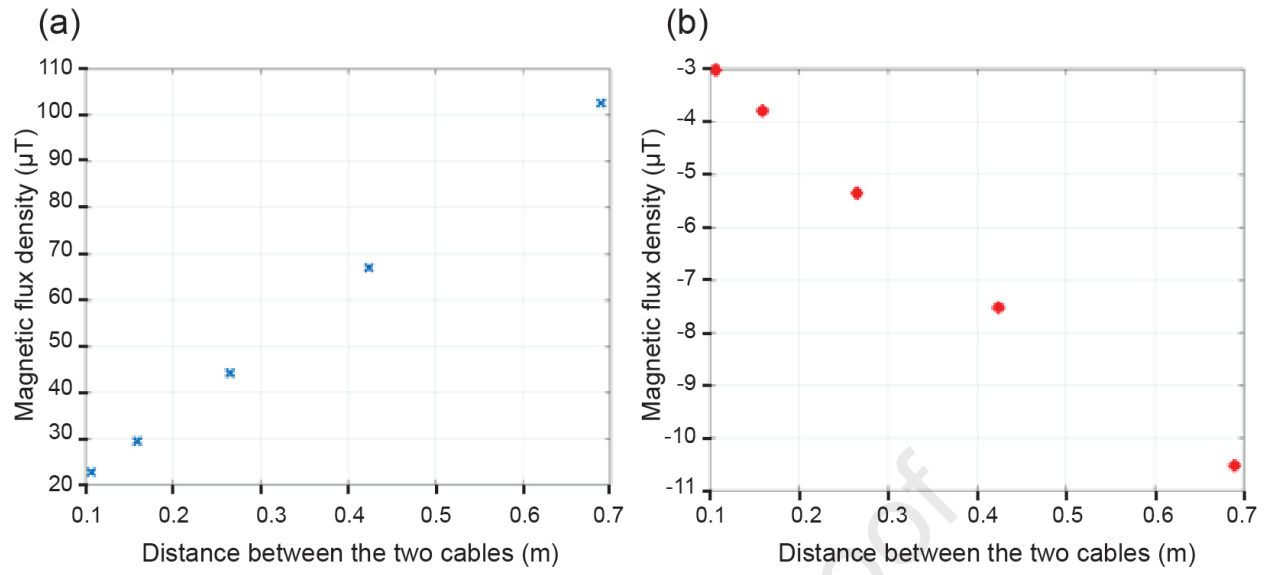
689

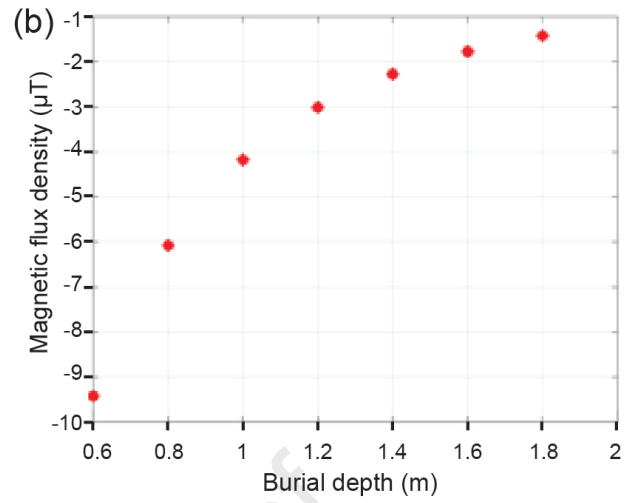
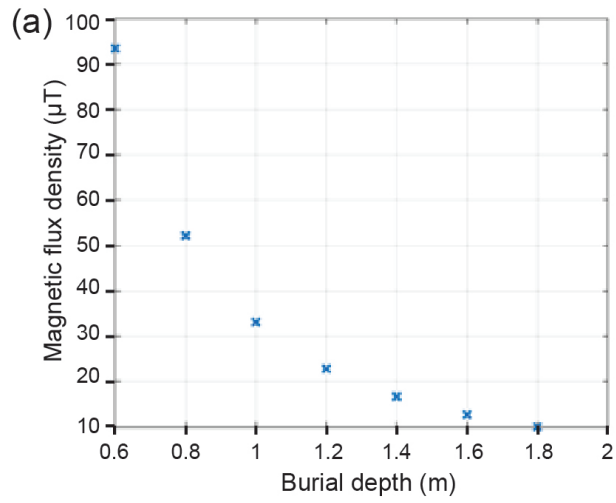
690 **CREDIT statement**

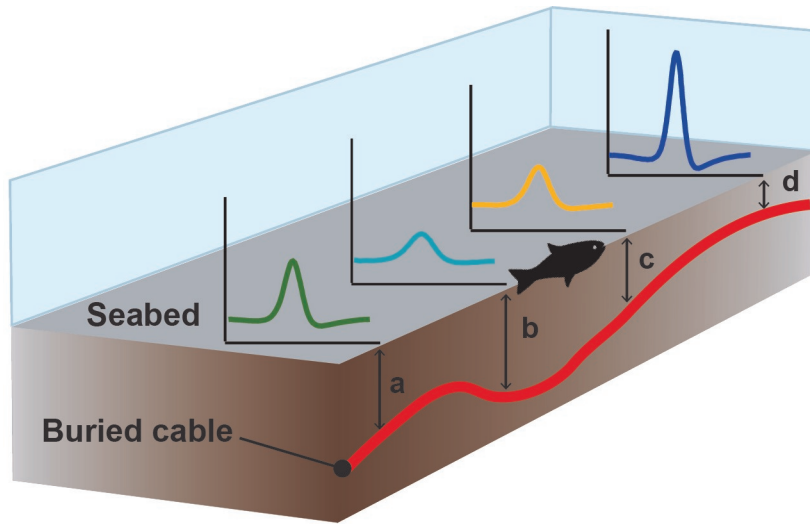
691 ZLH: Conceptualisation, writing - original draft, interpretive modelling. ABG: Conceptualisation,
692 interpretative modelling, writing - review & editing. PS: Interpretative modelling, writing - review &
693 editing. HH: Computational modelling, writing - review & editing. JWK: Supervision, funding
694 acquisition, project administration, writing - review & editing.



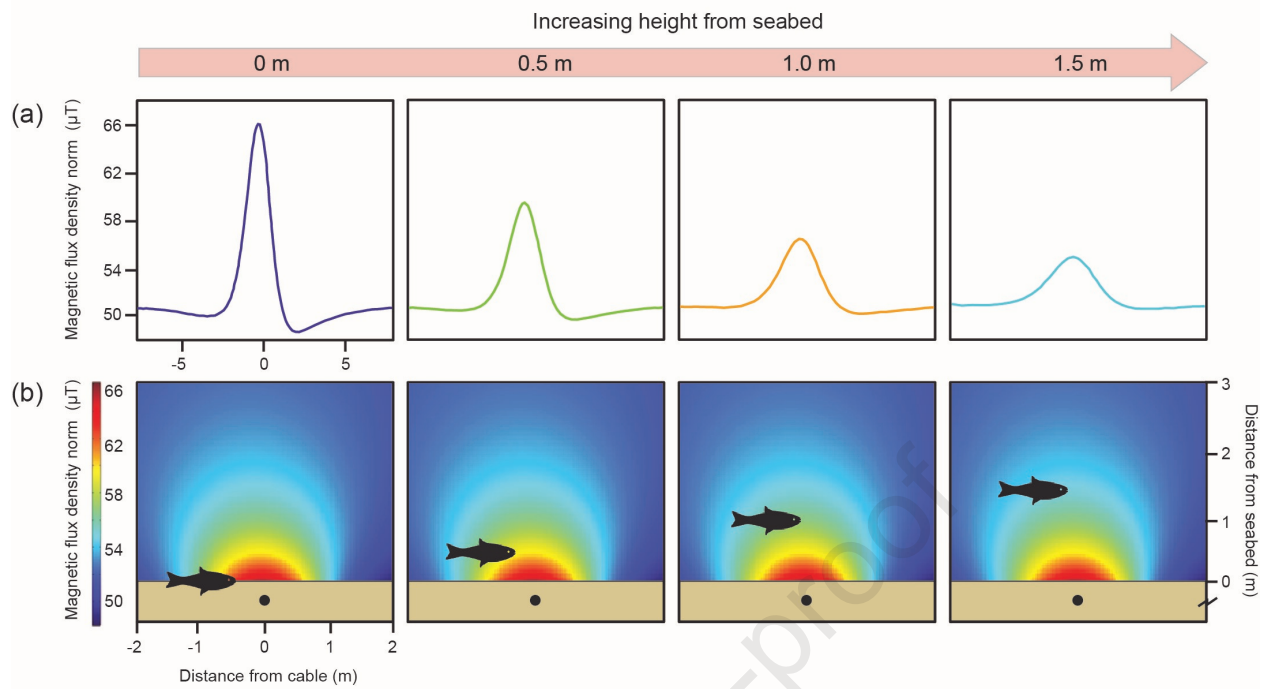
Journal Pre-proof







Journal Pre-proof



Highlights

1. In a bundled DC cable, closer cable cores reduced the emitted DC magnetic field (DC-MF) intensity
2. As a cable's burial depth increased, the intensity of DC-MF at the seabed surface decreased
3. Buried cables still present a DC-MF at intensities perceivable to some receptive species
4. Variable burial depth along a cable route will present a variable EMF to receptive species
5. An animal's proximity to a cable (buried or not) influences their exposure to the EMF

Declaration of interests

The authors declare that they have no known competing financial interests or personal relationships that could have appeared to influence the work reported in this paper.

The authors declare the following financial interests/personal relationships which may be considered as potential competing interests:

Journal Pre-proof